J Mater Sci (2012) 47:2328–2332
DOI 10.1007/s10853-011-6048-9

One-step hydrothermal synthesis of Li_2FeSiO_4/C composites as lithium-ion battery cathode materials

Meng Zhang · Qiuping Chen · Zhixia Xi · Yonggai Hou · Qiuling Chen

Received: 11 July 2011 / Accepted: 13 October 2011 / Published online: 29 October 2011

Abstract Li_2FeSiO_4/C composites were one-step synthesized under hydrothermal conditions at 200 °C for 72 h using glucose as carbon source. By adjusting the quantity of added glucose, we obtained varied Li_2FeSiO_4/C composites with different size and morphology. A series of electrochemical tests demonstrate that the Li_2FeSiO_4/C nanoparticles with diameters about 20 nm have higher discharge capacity, and slower capacity fading in comparison with Li_2FeSiO_4 and other Li_2FeSiO_4/C composites. Li_2FeSiO_4/C nanoparticles deliver a discharge capacity of 136 mAh g^{-1} at 0.2 C, and after 100 cycles, the discharge capacity remains 96.1%. Furthermore, Li_2FeSiO_4/C nanoparticles also exhibit an excellent rate capability with a capacity of about 80 mAh g^{-1} at 10 C.

Introduction

Recently, lithium-ion batteries have attracted significant interest because of their unique advantages [1–5], such as high energy density, high voltage, low self-discharge rate, low maintenance, and low toxicity. Apart from the wide application in portable equipment, Li-ion batteries are also considered to the most promising power sources for electric vehicles [6]. To meet the requirements of these expanding applications, the performance of Li-ion batteries needs to be further enhanced.

M. Zhang (✉) · Y. Hou
School of Materials Science and Engineering, Henan University of Technology, Zhengzhou 450007, China
e-mail: meng_zhang@haut.edu.cn

Q. Chen · Z. Xi · Q. Chen
Materials Science and Chemical Engineering Department, Politecnico di Torino, Corso Duca degli Abruzzi 24, 10129 Turin, Italy

Cathode materials are of vital importance to enhance the performance properties of batteries (especially energy density and cyclability) [7–9]. As one of the new cathode materials, Li_2FeSiO_4 possesses low cost, environmental friendliness, high safety, and electrochemical stability over conventional lithium transition metal oxides cathode materials [10–12]. Nevertheless, Li_2FeSiO_4 also exhibits poor electronic conductivity and lifetime, which limit its practical application. So far, various methods have been developed to optimize the electrochemical properties of Li_2FeSiO_4, for example, controlling the particle size and morphology [13, 14], doping certain cations [15, 16] and surface coating with conductive materials [17, 18]. Among these methods, carbon coating has been widely focused [19–21], because it not only improves electronic conductivity but also reduces the particle size, both of which are favorable to the transfer of electrons and ions.

In previous reports, Li_2FeSiO_4/C composites have been obtained by several different synthesis techniques, such as solid-state reaction [19], sol–gel method [20] and solution-polymerization [21]. However, these methods generally require high temperature or multi-step processing, which may result in carbon can not effectively contact Li_2FeSiO_4 and make products' electrochemical properties are unexpected [9].

Herein, we design a one-step hydrothermal strategy to prepare Li_2FeSiO_4/C composites under mild conditions. Electrochemical tests indicate the composites have higher discharge capacity, better rate performance, lower capacity fading, and interfacial impedance than Li_2FeSiO_4.

Experimental

In a typical procedure, 1 mmol $Fe(CH_3COO)_2{\cdot}4H_2O$, 2.3 mmol $Li(CH_3COO)_2{\cdot}2H_2O$, 1 mmol SiO_2 (Cabosil),

and 0.4 mmol glucose were mixed and dispersed in 40 mL distilled water in a 60 mL Teflon liner at room temperature. After stirred for few minutes, the liner was sealed in a stainless steel autoclave, and kept at 200 °C for 72 h, and then being cooled to room temperature naturally. The product was centrifuged and washed with distilled water and absolute ethanol several times, until dark brown precipitate was collected. Finally, the obtained product was dried in vacuum at 50 °C for 6 h. For comparison, Li_2FeSiO_4 was also prepared without the addition of glucose.

The phase structure of samples was examined by Powder X-ray diffraction (XRD; Philips X'pert MPD with Cu Kα radiation, $\lambda = 1.5418$ Å). The morphology and size of samples were analyzed by field emission scanning electron microscopy (FESEM; JSM-6700F). The specific surface areas of samples were evaluated from nitrogen adsorption data (Gemini V2380).

Electrochemical tests were conducted with coin cells (type 2016). The cathode was fabricated by pasting 80 wt% active material, 10 wt% acetylene black, and 10 wt% polyvinylidene fluoride (PVDF) dissolved in *N*-methylpyrrolidone (NMP) onto Al foil by doctor blade technique, and then the foil was dried under vacuum at 100 °C for 12 h. Metallic lithium was used as the anode. The electrolyte was 1 M $LiPF_6$ in a 1:1 mixture of ethylene carbonate (EC)/dimethyl carbonate (DMC); the separator was Celgard 2400. All the cells were assembled in a glove box filled with pure argon. The cells were cycled on an Arbin BT2043 battery test system between 1.5 and 4.5 V versus Li^+/Li. Electrochemical impedance spectra (EIS) were recorded by using a CHI660D electrochemical workstation in the frequency range of 10^{-1}–10^5 Hz.

Results and discussion

The XRD patterns of the as-prepared samples are shown in Fig. 1. The major peaks of both samples are well assigned to the orthorhombic phase Li_2FeSiO_4 (space group $Pmn2_1$) [10], and the impurities are mainly Fe_3O_4 and Li_2SiO_3. Compare to Li_2FeSiO_4 (Fig. 1a), the Li_2FeSiO_4/C (Fig. 1b) exhibits broader peak widths and weaker peak intensities, which reveals the existence of carbon restricts the growth and crystallization of Li_2FeSiO_4 particles. In addition, no diffraction peak of graphite can be clearly identified, indicating the carbons are mainly amorphous. It can be clearly observed the amorphous carbon bump in the small angle region (inset in Fig. 1).

Figures 2a and b give the FESEM images of Li_2FeSiO_4 and Li_2FeSiO_4/C composites, respectively. The two products are both nanoparticles. From Fig. 2a, one can see the Li_2FeSiO_4 particles are irregular polyhedrons, whose sizes are in the range of 30–110 nm. Correspondingly,

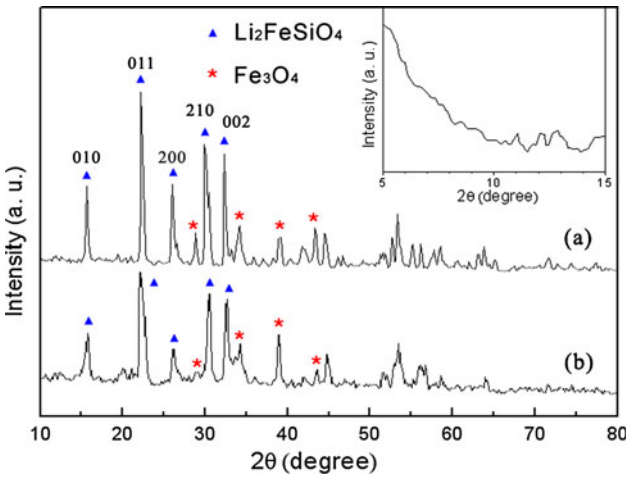

Fig. 1 XRD patterns of the as-prepared samples: *a* Li_2FeSiO_4 and *b* Li_2FeSiO_4/C

Li_2FeSiO_4/C composites have spherical morphology, with the average diameter of ca. 20 nm, displaying a relatively narrow size distribution. The reduction of particle sizes accords with the results XRD.

In our reaction system to fabricate Li_2FeSiO_4/C composites, the carbon roots in the carbonization of glucose under hydrothermal conditions: $C_6H_{12}O_6 \rightarrow 6C + 6H_2O$ [22]. Logically, the quantity of glucose can impact on the morphology and size of products. When the quantity of glucose was decreased to 0.1 mmol, only small amount of Li_2FeSiO_4/C nanoparticles are found. Figure 3a displays most of products are still irregular Li_2FeSiO_4 grains in this case. The yield of Li_2FeSiO_4/C composites continuously rises with the quantity of glucose from less to more. When 0.4 mmol glucose was added into reaction system, the yield of Li_2FeSiO_4/C nanoparticles would reach maximum (Fig. 2b). Afterward, glucose will bring excessive carbons, which tend to accumulate into larger grains (Fig. 3b).

Figure 4 illustrates a probable mechanism for the formation of Li_2FeSiO_4/C nanoparticles. The neonatal Li_2FeSiO_4 seeds are covered by the carbon coatings (arising from the carbonization of glucose), which block the crystallization and growth of these seeds, ultimately generating Li_2FeSiO_4/C nanoparticles.

As listed in Table 1, the data derived from N_2 adsorption give the BET surface area (S_{BET}) of samples. Li_2FeSiO_4/C composites with 0.4 mmol glucose (sample C) have the highest S_{BET}, which is consistent with the smallest particle size observed by FESEM.

The charge–discharge curves (second cycle) for the samples at 0.2 C between 1.5 and 4.5 V are shown in Fig. 5. All the samples have similar voltage profiles with the potential plateaus at around 2.8 V (charge) and 2.5 V (discharge), which correspond to the Li^+ ions deintercalation and intercalation process [10, 23]. The three

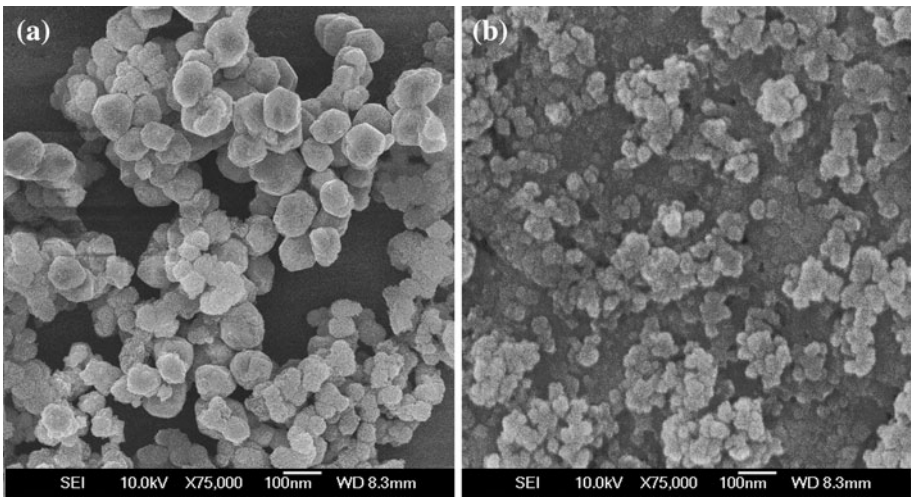

Fig. 2 FESEM images of the as-prepared samples: **a** Li_2FeSiO_4 and **b** Li_2FeSiO_4/C

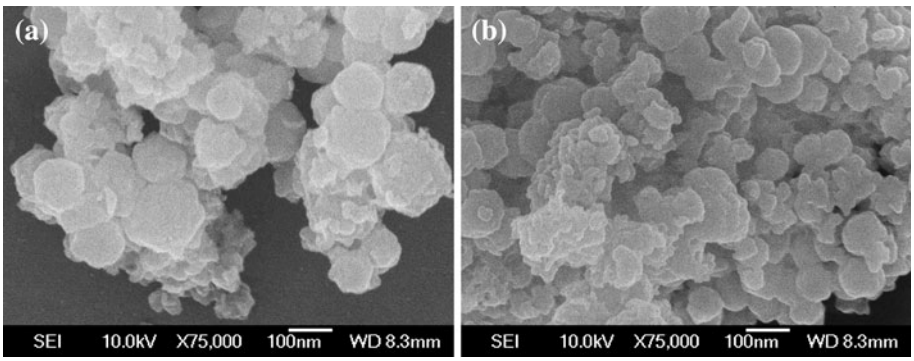

Fig. 3 FESEM images of the Li_2FeSiO_4/C samples prepared with **a** 0.1 mmol glucose and **b** 1.6 mmol glucose

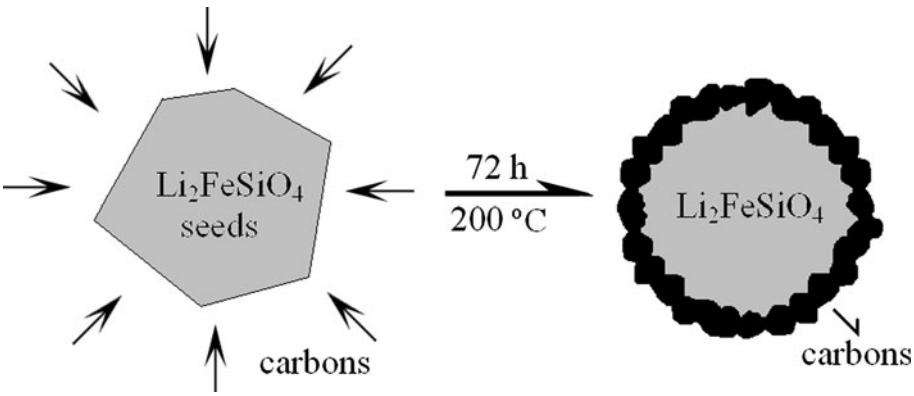

Fig. 4 Schematic illustration of the formation mechanism for Li_2FeSiO_4/C nanoparticles

Table 1 Specific surface area of the samples prepared with the different quantity of glucose

Samples	Glucose (mmol)	BET surface area ($m^2\ g^{-1}$)
A: Li_2FeSiO_4	0	18.5
B: Li_2FeSiO_4/C	0.1	54.2
C: Li_2FeSiO_4/C	0.4	98.5
D: Li_2FeSiO_4/C	1.6	79.3

Li_2FeSiO_4/C composites (sample B, 103 mAh g^{-1}; C, 136 mAh g^{-1}; and D, 92 mAh g^{-1}) deliver higher discharge capacity than that of Li_2FeSiO_4 (sample A, 68 mAh g^{-1}), which is mainly attributed to the following reasons. First, carbons decrease the particles' size and increase their specific surface area, which are in favor of the intercalation and deintercalation of Li^+ ions owing to a shortening of the ion diffusion path in cathodes [19, 24]. Second, Li_2FeSiO_4 particles are connected by carbons and form the conductive networks, which are helpful for the electron transfer [25]. Third, there are lots of interface structures between Li_2FeSiO_4 and carbons, and Li^+ ions can be freely intercalated in the interface structures during the discharging process; that enhances the amount of intercalated Li^+ ions and improves the discharge capacity

[26]. In addition, carbon is not active cathode materials, and thus too thick carbon coating will degrade the electrode capacity (sample D).

Figure 6 represents the cycle performance of the samples at 0.2 C between 1.5 and 4.5 V. Li_2FeSiO_4/C composites appear better capacity retention during cycling than that of Li_2FeSiO_4. In particular, sample C can maintain 96.1% of the highest discharge capacity after 100 cycles, with an average capacity fading of 0.053 mAh g^{-1} per cycle. Such an improvement in the cycle performance of the Li_2FeSiO_4/C composites over Li_2FeSiO_4 can be attributed to the existence of the carbon coating, which prevents direct contact between the active cathode materials and the electrolyte, and thus slow down the erosion of Li_2FeSiO_4 upon cycling [27]. Note the discharge capacity of samples continuously increases in the initial several cycles. This phenomenon maybe results from the activation of Li_2FeSiO_4, which are in the inner sites of cathode particles.

The rate performance of Li_2FeSiO_4 (sample A) and Li_2FeSiO_4/C composite (sample C) has been shown in Fig. 7. It is obvious that the Li_2FeSiO_4/C composite exhibits an excellent discharge capability in any measured rate, with a capacity of 136, 123, 113, 104, 90, and 80 mAh g^{-1} at 0.2, 0.5, 1, 2, 5, and 10 C, respectively. In contrast, the discharge capacity of Li_2FeSiO_4 is only 66, 51, 40, 30, 17, and 7 mAh g^{-1} at 0.2, 0.5, 1, 2, 5, and 10 C, respectively. It is not yet to fully understand why carbon coating can improve the electrode's rate performance. In our opinion, the following reasons are crucial: (1) carbon improves the cathode's electronic conductivity, which is the rate-limiting factor at low rates; (2) carbon reduces the size of Li_2FeSiO_4 particles and hence shortens the lithium ion diffusion path, which is the rate-limiting factor at high rates.

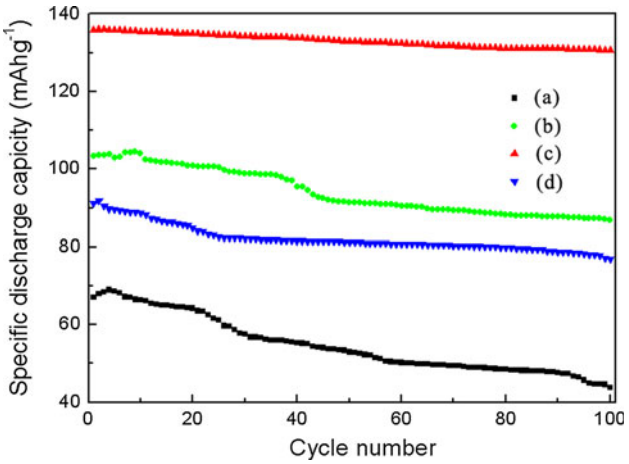

Fig. 6 Cyclic performance of *a* Li_2FeSiO_4 (sample A) and (*b–d*) Li_2FeSiO_4/C (sample B, C and D) at 0.2 C

To verify the above speculation, the EIS of Li_2FeSiO_4 (sample A) and Li_2FeSiO_4/C composite (sample C) has been investigated and shown in Fig. 8. Both profiles can be divided into three regions: (1) the high frequency semicircle is related to the of Li-ion diffusion in the surface film of the electrode; (2) the middle frequency semicircle indicates the charge transfer resistance (R_{ct}), which is related to the charge transfer at the interface between the surface film and electrode material; (3) the low frequency straight line is related to the Li-ion diffusion in the electrode material. For the Li_2FeSiO_4/C composite, the intercepts at the Z' axis are less than those of Li_2FeSiO_4, i.e., Li_2FeSiO_4/C have lower resistance than Li_2FeSiO_4, e.g., the R_{ct} value of the Li_2FeSiO_4/C composite is 179 Ω, while the R_{ct} value of the Li_2FeSiO_4 is 262 Ω. The relative information on the Li-ion diffusion may be obtained according to the following equation [24, 28].

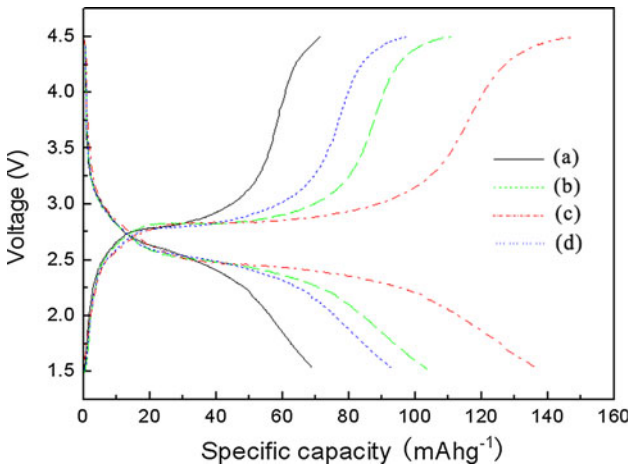

Fig. 5 The second charge–discharge curves of *a* Li_2FeSiO_4 (sample A) and (*b–d*) Li_2FeSiO_4/C (sample B, C and D) at 0.2 C

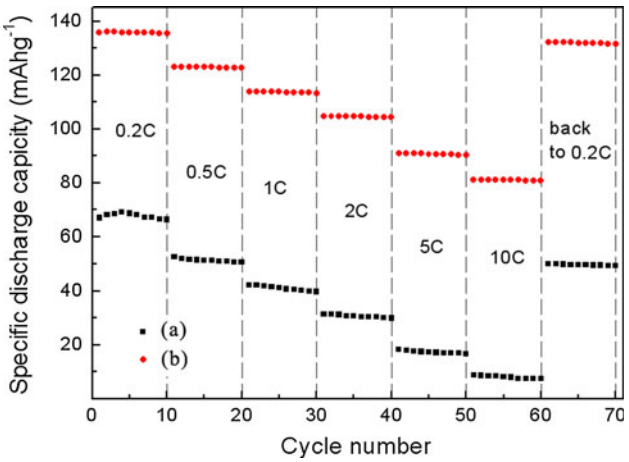

Fig. 7 Rate performance of *a* Li_2FeSiO_4 (sample A) and *b* Li_2FeSiO_4/C (sample C)

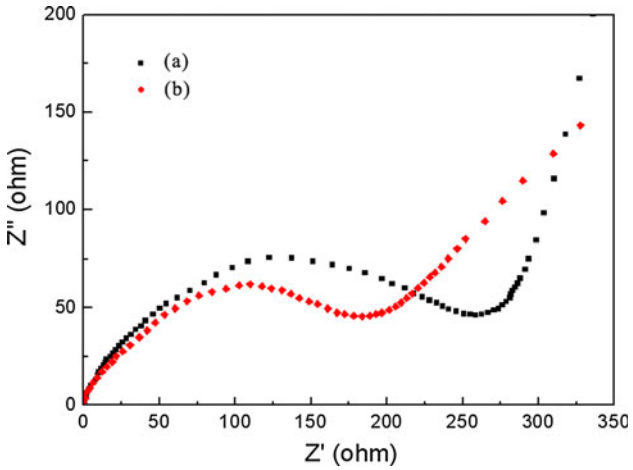

Fig. 8 EIS (Nyquist plots) of *a* Li_2FeSiO_4 (sample A) and *b* Li_2FeSiO_4/C (sample C)

$$D = R^2T^2/2A^2n^4F^4C^2\sigma^2 \quad (1)$$

where D is Li-ion diffusion coefficient, R is the gas constant, T is the absolute temperature, A is the surface area of the cathode, n is the number of electrons per molecule during oxidation, F is the Faraday constant, C is the concentration of Li-ion, and σ is the Warburg factor. The Li-ion diffusion coefficients of Li_2FeSiO_4/C composite and Li_2FeSiO_4, calculated from above equation are 9.71×10^{-11} and 2.32×10^{-12} cm^2 s^{-1}. It is the convictive evidence that the carbon coating enhances the Li-ion diffusion and electronic conductivity.

Conclusions

Li_2FeSiO_4/C composites have been synthesized through a convenient one-step hydrothermal method under mild conditions. Electrochemical tests indicate Li_2FeSiO_4/C has higher discharge capacity, lower capacity fading and better rate performance than Li_2FeSiO_4. The improvement of electrochemical performance can be attributed to the presence of carbon coating, which control the size and specific surface area of Li_2FeSiO_4, prevents the Li_2FeSiO_4 from the direct contact with the electrolyte and increases the Li-ion diffusion and electronic conductivity.

Acknowledgements This study was supported by Zhengzhou Key Laboratory for Clean Energy (111PYFZX151).

References

1. Scrosati B, Garche J (2009) J Power Sources 195:2419
2. Marom R, Amalraj SF, Leifer N, Jacob D, Aurbach D (2011) J Mater Chem 21:9938
3. Bruce PG, Scrosati B, Tarascon JM (2008) Angew Chem Int Ed 47:2930
4. Li Z, Zhang D, Yang F (2009) J Mater Sci 44:2435. doi: 10.1007/s10853-009-3316-z
5. Kushnir D, Sandéna BA (2011) J Clean Prod 13:1405
6. Kazunori O (2009) Lithium ion rechargeable batteries: materials technology and new applications. Wiley-Vch, Weinheim
7. Wang Y, Cao G (2008) Adv Mater 20:2251
8. Sun YK, Myung ST, Park BC, Prakash J, Belharouak I, Amine K (2009) Nat Mater 8:320
9. Ellis BL, Lee KT, Nazar LF (2010) Chem Mater 22:691
10. Nytén A, Abouimrane A, Armand M, Gustafsson T, Thomas JO (2005) Electrochem Commun 7:156
11. Peng ZD, Cao YB, Hu GR, Ke D, Xu GG, Zheng WX (2009) Chin Chem Lett 20:1000
12. Sirisopanaporn C, Masquelier C, Bruce PG, Armstrong AR, Dominko R (2011) J Am Chem Soc 133:1263
13. Dominko R, Conte DE, Hanzel D, Gaberscek M, Jamnik J (2008) J Power Sources 178:842
14. Song HK, Lee KT, Kim MG, Nazar LF, Cho J (2010) Adv Funct Mater 20:3818
15. Dominko R, Sirisopanaporn C, Masquelier C, Hanzel D, Arcon I, Gabersceka M (2010) J Electrochem Soc 157:A1309
16. Deng C, Zhang S, Yang SY, Fu BL, Ma L (2011) J Power Sources 196:386
17. Li C, Zhang HP, Fu LJ, Liu H, Wu YP, Rahm E, Holze R, Wu HQ (2006) Electrochim Acta 51:3872
18. Chen Z, Qin Y, Amine K, Sun YK (2010) J Mater Chem 20:7606
19. Huang X, Li X, Wang H, Pan Z, Qu M, Yu Z (2010) Solid State Ion 181:1451
20. Fan XY, Yan Li, Wang JJ, Lei G, Peng Z, Li DL, Huang L, Sun SG (2010) J Alloys Compd 493:77
21. Lv D, Wen W, Huang X, Bai J, Mi J, Wu S, Yang Y (2011) J Mater Chem 21:9506
22. Mi Y, Hu W, Dan Y, Liu Y (2008) Mater Lett 62:1194
23. Nytén A, Kamali S, Häggström L, Gustafssona T, Thomas JO (2006) J Mater Chem 16:2266
24. Zhang S, Deng C, Fu BL, Yang SY, Ma L (2010) J Electroanal Chem 644:150
25. Huang X, Li X, Wang H, Pan Z, Qu M, Yu Z (2010) Electrochim Acta 55:7362
26. Zhang M, Yan G, Hou Y, Wang C (2009) J Solid State Chem 182:1206
27. Li YD, Zhao SX, Nan CW, Li BH (2011) J Alloys Compd 509:957
28. Shenouda AY, Liu HK (2008) J Power Sources 185:1386